NBSIR 78-1495

Factors Affecting the Durability of Adobe Structures

Paul Wencil Brown[1]
Carl R. Robbins[2]
James R. Clifton[1]

[1]Center for Building Technology
National Engineering Laboratory
National Bureau of Standards
Washington, D.C. 20234

[2]Center for Materials Research
National Measurement Laboratory
National Bureau of Standards
Washington, D.C. 20234

July 1978

Prepared for
National Park Service
Washington, D.C. 20240

NBSIR 78-1495

FACTORS AFFECTING THE DURABILITY OF ADOBE STRUCTURES

Paul Wencil Brown[1]
Carl R. Robbins[2]
James R. Clifton[1]

[1]Center for Building Technology
National Engineering Laboratory
National Bureau of Standards
Washington, D.C. 20234

[2]Center for Materials Research
National Measurement Laboratory
National Bureau of Standards
Washington, D.C. 20234

July 1978

Prepared for
National Park Service
Washington, D.C. 20240

U.S. DEPARTMENT OF COMMERCE, Juanita M. Kreps, *Secretary*

Dr. Sidney Harman, *Under Secretary*

Jordan J. Baruch, *Assistant Secretary for Science and Technology*

NATIONAL BUREAU OF STANDARDS, Ernest Ambler, *Director*

TABLE OF CONTENTS

ABSTRACT

Adobe samples from three structures of historic interest in the state of Arizona were analyzed to determine their mineral assemblages, particle size distributions, soluble salt contents, and porosities. These analyses were accompanied by microscopic observations of polished sections and thin sections. These data were correlated with the weathering observed and it was found that soluble salt action was primarily responsible for the deterioration of the adobe from one of the sites The nature of the particle size distribution has contributed to the rapid deterioration of the adobe from a second site. The adobe from a third site was found to be well consolidated due to the presence of large amounts of calcite.

FACTORS AFFECTING THE DURABILITY OF ADOBE STRUCTURES

by
Paul Wencil Brown
Carl R. Robbins
James R. Clifton

1. INTRODUCTION

A large number of adobe and rammed earth structures have been built in the southwestern United States over a period of approximately 10 centuries. Due to the scarcity of more conventional building materials and the climatic conditions prevalent in the region, adobe was the primary material of construction employed. Adobe is a mixture of sand, silt, and clay, however, straw is usually added and gravel is usually present. Sand may also be added to an adobe soil to achieve the desired proportions [1][1/]. When mixed with water, adobe can be cast into brick or block, cast in-place, or used as mortar. Adobe exhibits excellent stability in climates of extreme dryness as is evidenced by the antiquity of Middle Eastern adobe structures such as the Ziggurat of Agar Quf. However, exposure of an adobe structure to moisture, whether from rain, rising ground water or high humidity, causes deterioration generally called weathering. The rate at which adobe weathers is affected by its mineralogical composition, particle size distribution, porosity distribution and soluble salt content as well as its moisture content. Major weathering processes include erosion or leaching of the silt-clay matrix, soluble salt action, dimensional instability associated with cyclic wetting and drying, and freeze-thaw damage [1].

It is the purpose of this paper to examine the factors which affect the weathering of adobe.

2. SELECTION OF MATERIALS

Adobe material was obtained from three sites in the state of Arizona. These sites are Tumacacori National Monument, Fort Bowie National Historic Site, and Escalante Ruin. Tumacacori National Monument is a mission church, San José de Tumacacori, and other buildings constructed by Franciscan priests in the late 18th century. The church was abandoned in 1848 and fell into disrepair until 1921. Since then, repair work has been essentially limited to preserving the existing structure. Fort Bowie was a cavalry fort first constructed in 1866. A second fort was built in 1868 and was in use for the next 16 years and then abandoned. Escalante Ruin is the remains of a prehistoric farming community built along the Gila River. This site was occupied for several centuries and many of the artifacts excavated date from A.D. 1150-1450; however, portions of the site date as early as A.D. 900.

[1/] Numbers in brackets refer to references at the end of this report.

The samples of adobe taken from Tumacacori ranged from well consolidated to severely deteriorated. A sample of soil from the site was also obtained. Three samples were taken from various locations along an interior wall of the nave of the church and showed varying degrees of deterioration. One sample, considered to be representative of unweathered adobe, was taken from an interior wall of the sanctuary. In addition other samples were taken from the top of an exposed wall, and from the exterior wall of the nave. The sample of adobe from Fort Bowie was taken from a severely deteriorated corral wall. The sample from the Escalante Ruin was taken from the wall of a dwelling unit and was well consolidated. The appearance of a typical polished section of each adobe included in this investigation is shown in Figure 1.

3. ANALYTICAL RESULTS

3.1 Escalante Ruin

3.1.1 General Observations and Visual Analysis

Escalanate adobe is well consolidated, pinkish gray in color (Munsell soil chart notation 7.5 yr 7/2)[2] and appears to contain a high percentage of fine fraction relative to coarse aggregate. The latter consists primarily of angular to subrounded quartz grains and rounded residual fragments of highly weathered igneous rock (granites) in which the feldspar has been altered to clays. The light color of the specimen suggested the presence of a carbonate which was confirmed by reaction with dilute hydrochloric acid. The carbonate, found to be calcite, is present in considerable concentration and is distributed throughout the sample.

This adobe is predominantly fine grained and dense, with an even distribution of relatively large pores (1-2 mm diameter). Subsamples of a larger Escalante specimen showed considerable variation in their resistance to the destructive effects of water. Although ~75% of these subsamples were quite resistant, the remainder dissociated readily when immersed in water, reflecting a significant variation within a relatively small sample volume.

Examination of an epoxy impregnated polished section of this adobe in reflected white light shows an aggregate fraction ~5mm in its largest dimension (Figure 2). This size fraction consists mainly of rounded to subangular clear and milky quartz grains, and grains of feldspars. In the finer fractions the angularity of the aggregate rapidly increases with decreasing aggregate size. In addition to quartz and feldspars, amphibole, chlorite, and titanite are observed. The calcium carbonate occurs as a finely crystalline white material deposited between the finer grains, as a filling in the smaller pores, and as a lining of the larger pores. It is both a cementing agent and a pigment, whose presence results in a light colored adobe.

A petrographic thin section, prepared after impregnating the adobe with epoxy, was examined in polarized light[2]. The outstanding feature of the material is its microcrystalline calcite-clay matrix which surrounds the larger grains and serves as the cementing agent of the adobe (Figure 3). A variety of quartz grains are present. These range from small angular individual fragments to large aggregate material which is frequently strained, polycrystalline and rounded in habit. Both alkaline (microcline, orthoclase) and calcic feldspars are abundant. Much of the feldspar is chemically unaltered, but some of the plagioclase has been extensively weathered to clay. In addition, amphibole, chlorite and the iron oxides hematite and magnetite are present in minor amounts.

3.1.2 Soluble Salt Analysis

Qualitative elemental analysis of the soluble salt fraction was obtained with a scanning electron microscope (SEM) equipped with an energy dispersive x-ray analysis (EDXA) attachment. The soluble salt fraction was obtained by dispersing the adobe in distilled water, filtering the liquid, evaporating it to dryness and collecting the salt as the residue[2]. The elements identified by this method in apparent order of abundance are: Ca, Cl, S, Si, and trace amounts of Mg, K, and Al. The energy distribution spectrum of this fraction obtained by EDXA is shown in Figure 4. This spectrum typifies the EDXA data obtained in the analyses of soluble salts present in other samples.

3.1.3 X-ray Diffraction Analysis

A 100 gram subsample of the Escalante specimen was analyzed using x-ray diffractometry in order to obtain an estimate of the relative abundance of the various minerals present in the bulk sample[2]. The following minerals, listed in apparent order of abundance, were identified as calcite, quartz, microcline, plagioclase, orthoclase and illite.

3.1.4 Particle Size Distribution Analysis

The particle size distribution in a 260 gram sample was determined using sieving and sedimentation techniques[2]. The soluble salt content determination was carried out on a companion sample. These data along with x-ray diffraction analysis data for the various size fractions are reported in Table 1. The minerals described in this table are listed in decreasing order of abundance. Quartz, feldspars, calcite, and mica are the major components of the gravel and sand fractions while the major components of the silt and clay size fractions are calcite, illite, and quartz. Calcite, because of its insolubility and cementing properties, is not sensitive to the usual dispersion techniques and as a consequence, was observed in virtually all size fractions.

The coarse fractions (4-50 mesh) of the adobe specimen from Escalante Ruin consist primarily of a complex of igneous mineral and rock fragments

Table 1. Summary of Analysis of Escalante Adobe

Size Fraction Mesh Per Ince (U.S. Standard)	Percent of Sample Weight	X-ray Analysis	Remarks
Gravel:			
+4	4.35		Subangular to rounded grains of quartz, very altered granite, 2-feldspar biotite granite (little altered), quartzite, schist
-4 +8	4.93		" "
Sand:			
-8 +16	4.62		" "
-16 +30	4.59	Quartz, feldspars, calcite, mica	Flakes of chemically altered biotite mica observed
-30 +50	6.21	" "	" "
+50 +100	10.00	Quartz, feldspars, calcite, mica (trace)	Quartz and feldspars are the major minerals
-100 +200	11.55	Quartz, feldspars, calcite, mica	" "
-200 +270	11.28	" "	" "
-270 +400	6.38	Quartz, calcite, feldspars, trace of illite clay-mica	Quartz is the major mineral and most angular of the group
-400 +20μm	13.18	Quartz, calcite, feldspars, illite clay-mica	Quartz and calcite are the major minerals
Silt (-20μm +2μm)	15.37	Calcite, mixed layer clay minerals, predominantly illite, quartz, feldspars	Calcite/illite ratio much higher than in clay fraction
Clay (<2μm)	6.08	Calcite, mixed layer clay minerals, predominately illite, quartz	Calcite is the major mineral
Organic	Nil		
Soluble Salts	1.6		Primarily calcium chloride and gypsum

(granites). The morphology of the grains in this fraction ranges from angular to rounded. Quartz is prominent and occurs as rose, milky or colorless grains. Individual fragments of chemically unaltered feldspar crystals are present as are angular fragments of a granite. Grains of a second type of granite are rounded and its feldspars are highly weathered to clays. Occasional rounded grains of quartzite and schist are observed along with grains of calcite. Minor minerals present are an amphibole, chlorite, weathered biotite mica, and titanite. Below 50 mesh, the rock fragments become less prominent and from -50 to +270 mesh, the mineral assemblage, in order of decreasing abundance, consists of quartz, feldspars, microcrystalline calcite grains and mica. From -270 mesh to +2μm, calcite replaces the feldspars as the second most abundant mineral and small amounts of illite clay-mica appear in the x-ray diffractograms. Calcite is the major mineral in the silt fraction and is present mainly in microcrystalline form. A mixed layer, predominantly illitic, clay is present along with quartz and feldspars. In this size fraction, only the quartz grains are angular. The minerals observed in the clay size fraction are calcite, which is a major component, a moderate amount of a mixed layer clay showing a broad (001) x-ray diffraction peak at ∿10.8 Å, and a small amount of quartz. The clay present is predominantly illite which is a dimensionally stable clay.

The clay-silt matrix is the bonding or cementing material of adobes. The clay which is slowly formed by chemical weathering, and which is present on the surfaces of all size fractions of feldspars also contributes to bonding. This is particularly true in the clay-silt size fraction which is composed of clay particles initially present plus those on the surfaces of the tiny grains of feldspars that are gradually being converted to clays.

3.1.5 Summary

The calcite-clay bonding matrix of Escalante adobe is its distinctive feature. The calcite-clay ratio is not uniform in the matrix, but ranges on a micro scale from regions rich in clay to those which are nearly pure calcite. The latter are very resistant to the eroding effects of water and account for the variability in slaking resistance observed. The presence of calcite accounts for both the color and the high degree of consolidation generally observed in this adobe.

3.2 Fort Bowie National Historic Site

3.2.1 General Observations and Visual Analysis

The specimen of adobe from an exterior corral wall of Fort Bowie National Monument analyzed is yellowish brown (10 yr. 5/4, Munsell soil chart notation) and highly porous with many fine pores and a high percentage of large ones ranging from ∿1mm to 3mm in diameter. Microstructural details of the adobe are obscured by a clay-silt coating of the grains. Gross structural details which may be observed are fragments of residual organic material such as grass or straw and a high percentage of coarse aggregate.

A distinctive feature of the Fort Bowie adobe observed in polished section is the high ratio of aggregate to fine matrix. The aggregate consists primarily of angular to subrounded grains of quartz and feldspars ranging from ∿0.3mm to ∿15mm in largest dimension. The general aspect of the material is shown in Figure 5.

Examination of a petrographic thin section in polarized light showed large mosaic quartz grains. Large feldspar grains including microcline and orthoclase, both unaltered and altered to clays, and plagioclase grains, both unaltered and altered to clays, were also observed. The grains were angular to subrounded in habit and this assemblage persisted over a wide size range. In addition to the major mineral assemblage, minor amounts of micas, amphibole, and hematite were observed. The dominant feature observed in thin section is the high ratio of relatively coarse grains to clay-silt matrix, Figure 6. The high proportion of large grains seperated and bonded by many narrow regions of silt-clay matrix is readily observed in this figure.

3.2.2 Soluble Salt Analysis

Only a small amount of soluble salts was found in this sample. Energy dispersive x-ray analysis was used to obtain a qualitative estimate of the elements present in the soluble salt fraction. Elements identified by this method, in apparent order of abundance, are: Ca, Si, K, S, Cl, and Mg.

3.2.3 X-ray Diffraction and Particle Size Distribution Analyses

A subsample of the Fort Bowie specimen was crushed, ground and thoroughly mixed for x-ray analysis of the bulk sample. The following minerals (Listed in apparent order of abundance) were identified: quartz, plagioclase, microcline, orthoclase, weathered muscovite, illite, magnetite and a trace of kaolinite. Table 2 lists the particle size distribution, soluble salt and mineralogical data for this adobe. The minerals are listed in decreasing order of abundance. Size distribution analyses revealed a high proportion of coarse aggregate. Over 25% of this material is gravel and nearly 60% is larger than 50 mesh.

The adobe from the Fort Bowie National Historic Site is composed primarily of fragments of igneous rocks and minerals bonded by a clay-silt matrix. The coarse aggregate (10-15mm in its longest dimension) is angular and consists mainly of granite fragments with weathered feldspars, quartz grains and occasional fragments of quartzite. Amphibole and magnetite are present in minor amounts.

With decreasing grain size the rock fragments are replaced by quartz and feldspars, and the assemblage of quartz, feldspars, and mica and magnetite persists through several size fractions to ∿20μm. At this point, illite and Kaolinite are detected by x-ray analysis. The proportion of these minerals increases with decreasing grain size as the clay size (<2 microns) is approached. The clay fraction in decreasing order of abundance consists of illite-mica, quartz, and kaolinite and is dimensionally stable.

Table 2. Summary of Analysis of Fort Bowie Adobe

Size Fraction Mesh Per Inch (U.S. Standard)		Percent of Sample Weight	X-ray Analysis	Remarks
Gravel:				
	+4	13.39		Large angular grains of igneous rocks (two feldspar granites). Some of the feldspars are highly altered to clays. Amphibole and magnetite present
-4	+8	12.12		" "
Sand:				
-8	+16	11.99		" "
-16	+30	11.06	Quartz, feldspars, magnetite, mica (trace)	As above with individual quartz grains more abundant
-30	+50	9.50	Quartz, feldspar, mica, magnetite	As above with individual quartz and feldspar grains more abundant
-40	+100	7.08	" "	Rock fragments decreasing. Quartz and feldspar grains predominant
-100	+200	6.47	" "	Quartz and feldspar are the major minerals
-200	+270	3.20	" "	" "
-270	+400	2.11	" "	" " Feldspar grains are angular to subrounded and show some degree of alteration to clays. Quartz grains are more angular
-400	+20μm	7.63	Quartz, feldspars, illite-mica, kaolinite (trace), magnetite (trace)	
Silt (-20μm	+2μm)	8.86	Quartz, illite-mica feldspars, kaolinite	
Clay (-2μm)		6.56	Illite-mica, quartz, kaolinite	
Organic		Nil		
Soluble Salts		0.03		

3.2.4 Summary

The large number of pores with diameters in the range of ~1 to 3mm (Figure 1) and the high ratio of coarse aggregate to bonding matrix (Figure 6 and Table 2) are distinctive features of the adobe from the corrals at Fort Bowie. These factors account for the severe deterioration of this structure over a relatively short time span. The high degree of porosity allows the intrusion of water which reduces the shear resistance of the silt-clay matrix to the point where it cannot resist the flow of the coarse aggregate which is present in high proportion.

3.3 Tumacacori National Monument

The locations of the adobe samples taken from Tumacacori National Monument, their identification codes, and their condition when sampled are indicated in Figure 7. An additional sample, To_{15}, is a soil sample taken from the N.E. corner of the grounds. Three of these specimens To_{18} (interior), To_{10} (exterior) and To_{15} (soil) were size fractionated and the size fractions were studied in detail. The remaining four samples were selected to investigate other aspects of this adobe.

3.3.1 General Observations and Visual Analysis

A typical specimen of Tumacacori adobe is dark brown (Munsell notation 7.5 yr 4/2). As in the case of the other adobes investigated, most of the structural detail is obscured by the fine matrix which coats the larger grains. This adobe has many fine pores. It also contains coarse pores ranging up to 4mm in diameter. Residual fragments of organic material (straw, grass or twigs) are preserved in the finer fraction of the adobe. This adobe is in general well-consolidated and contains a much lower proportion of coarse aggregate than the adobe from Fort Bowie. Occasional rounded to subrounded grains of quartz and granites are observed but most of the aggregate is not visible. Small white pore fillings of gypsum are present in several of the specimens. Calcite is also present.

Epoxy-impregnated polished sections of specimens To_{10}, To_{11}, To_{12}, To_{16}, and To_{18} were prepared for examination in reflected white light at low magnification. The general aspect of the material is shown in Figure 8. The large aggregate consists mainly of grains of quartz and chemically weathered granites. The angularity of the aggregate grains increases rapidly with decreasing grain size in the finer size fractions. The white material visible in many of the pores is gypsum.

Although gypsum was observed in all specimens, it was most abundant in speciment To_{11} which was taken from a wet area of the structure where ground water is active. Euhedral crystals of gypsum up to 3mm in their longest dimension were observed in a polished specimen of To_{11}.

These crystals were commonly interconnected by small gypsum filled veins or channels. The general aspect of the adobe from this sampling site may be seen in a photomicrograph of an unpolished surface, Figure 9. Examination of a petrographic thin section (To_{17}), which is typical of Tumacacori adobe, shows a fabric and mineral assemblage quite different from those of Escalante and Fort Bowie, and distinctive for this material. The coarse aggregate consists of both rounded and angular grains of quartz, rounded fragments of quartzite, euhedral crystals of unaltered alkaline feldspar, and angular to rounded grains of calcic feldspars, most showing chemical alteration to clay. In addition chlorite, hematite, muscovite, altered amphibole, gypsum and titanite are present in a clay-silt matrix. A distinctive feature of this adobe is the chemical zoning of the feldspars which is easily observed in polarized light, Figure 10.

3.3.2 X-ray Diffraction Analysis

Bulk x-ray powder diffraction patterns were taken of samples To_{10}, To_{11}, To_{12}, To_{15} and To_{17}. All patterns were quite similar, differing mainly in the relative proportions of the various minerals present. These differences, however, are not large and can probably be attributed to the proportioning of the adobe soil with sand during the construction of this structure. The nature of this proportioning is indicated by comparison of the particle distribution of the soil sample, To_{15}, with those of samples To_{10}, and To_{18} which were taken from the structure. The percentage weight of the silt-clay fractions in the soil sample is 83.3 while those of To_{10} and To_{18} are 23.9 and 18.1, respectively. This indicates that the soil to sand ratio used in proportioning adobe for Tumacacori was about 1 to 4. In addition the rounded aspect and the general absence of particle angularity of the grains in the coarser sand and gravel fractions of Tumacacori adobe indicates that the sand was subjected to abrasive action. Particles of this size tend to become rounded through the action of running water. This suggests that this material was obtained from a stream near the site.

The diffraction pattern of To_{12} shows the following minerals, listed in apparent order of abundance: quartz, alkaline and calcic feldspars, muscovite, amphibole, biotite, illite, and traces of kaolinite and gypsum. Sample To_{10} is very similar to To_{12} but contains more gypsum, sample To_{17} contains less muscovite, alkali feldspar, and amphibole, and sample To_{11}contains more alkali feldspar, less amphilobe and a much higher percentage of gypsum. Sample To_{15} (soil) contains much less muscovite, feldspar, and gypsum than the samples from the structure but shows a higher percentage of illite and kaolinite. In addition, the diffraction pattern of the soil sample shows a prominent peak at $\sim$14.7Å. This is characteristic of the (001) reflection of the montmorillonite group of clay minerals.

The clay size fraction (<2μm) was separated from five Tumacacori specimens by sedimentation. Both oriented and unoriented x-ray sample mounts were prepared. All samples were glycolated to test for the characteristic swelling of minerals of the montmorillonite group. Analytical results are given in Table 3. The minerals are listed in decreasing order of abundance.

Table 3. Major Minerals in the <2μm Fractions of Tumacacori Adobe

SPECIMEN NUMBER	ANALYTICAL RESULTS
To_{10}	Quartz, illite, feldspars
To_{12}	Quartz, illite, feldspars kaolinite
To_{15}	Quartz, illite, montmorillonite, feldspars, kaolinite
To_{17}	Quartz, illite, feldspars, mica, kaolinite
To_{18}	Quartz, illite, feldspars, montmorillonite

3.3.3 Particle Size Distribution Analysis

Specimens To_{10}, To_{18} and To_{15} were selected for size fraction analysis. Descriptions of the mineral and rock fragments of the various size fractions are given in Tables 4, 5 and 6. Components are listed in decreasing apparent order of abundance. The rock fragments of soil speciment To_{15}, are similar to those of To_{10} and To_{18}.

The organic matter observed in the adobe from Tumacacori consisted of twigs and what appeared to be fragments of grass or straw. In all instances there was a larger amount of organic matter present in adobe material from the structure than from the soil sample. While this is not a conclusive indication that it was added intentionally, this possibility cannot be excluded.

The adobe of Tumacacori is composed primarily of residual fragments of igneous rocks (granites) and their products of chemical weathering. However, the samples examined showed some variability on both the micro- and macro-scale. With decreasing grain size the weathered rock fragments are gradually replaced by individual mineral grains, primarily quartz and feldspars with minor amounts of mica, amphibole, magnetite, titanite, gypsum and perhaps calcite (-30 +50 mesh). At -270 +400 mesh, angular quartz is the dominant mineral and remains the major mineral with decreasing grain size even in the clay size fraction. The feldspar grains in the -270 +400 mesh fraction are subangular to rounded and chemically weathered with clay crystals on their surfaces. With further decreases in particle size, the percentages of true clay minerals gradually increase.

Quartz is the dominant phase in the clay size (<2μm) fraction of the five Tumacacori specimens studied (Table 3). The mineral assemblages are all quite similar. Traces of kaolinite, micas and montmorillonite are probably present in all samples but in amounts beyond the limits of detection by x-ray analysis.

The montmorillonite observed in the bulk samples of To_{15} and To_{18} has an (001) d-spacing of ∿14.7Å which expands to ∿17 Å with glycolation. It is present as a minor mineral in sample To_{18} but is present in sample To_{15} in amounts easily detectable by x-ray analysis, since the bulk soil sample contains a larger clay fraction than the samples from the structure.

Clay mineralogy affects the stability of adobe because of the marked effect of clay on the physical properties of soils and soil materials. In particular clay mineralogy affects expansion and variations in cohesiveness and plasticity of soils as a function of moisture content. These effects result primarily from the property of clay minerals to attract and hold water directly on the clay-particle surfaces. In the case of the swelling clays, such as montmorillonite, incorporation of interlayer water is accompanied by a large increase in volume. The amount of clay in Tumacacori adobe is relatively small (8-12 wt.%). Montmorillonite was detectable in only one of the adobe specimens from the structure (To_{18}) and is present in this specimen in only minor amounts. It may be concluded, therefore, that the effects of the presence of a swelling clay on the plysical properties of Tumacacori adobe are minor.

Table 4. Tumacacori (To_{10}) Size Fraction Analysis

Size Fraction Mesh Per Inch (U.S. Standard)	Percent of Sample Weight	X-ray Analysis	Remarks
Gravel:			
+	1.39		
-4 +8	3.79		Angular to subrounded grains of quartz and of weathered granites. Occasional rounded quartzite grains.
Sand:			
-8 +16	5.99		
-16 +30	8.57	Feldspars, quartz, mica, amphibole	Angular grains of weathered granites, many with biotite, angular to subrounded grains of clear and milky quartz.
-30 +50	9.52	" " "	Individual grains of feldspars and amphibole also present. Granite fragments decreasing in amounts.
-50 +100	8.48	Quartz, feldspars	" " "
-100 +200	8.26	Quartz, feldspars, mica, amphibole	" " "
-200 +270	6.79	" " "	" " "
-270 +400	6.45	Quartz, feldspars, mica, amphibole (trace)	Angular quartz is the dominant mineral. Feldspars and mica decreasing.
-400 +20μm	16.67	Quartz, feldspars, mica, illite amphibole (trace)	" " "
Silt (-20μm +2μm)	12.67	Quartz, feldspars, mica, and illite	" " "
Clay (<2μm)	11.24	Quartz, illite, feldspars	
Organic	0.18		Twigs, grass
Soluble Salts	1.26		Primarily $CaSO_4 \cdot 2H_2O$ and $CaCl_2$ (chlorides and sulfates of Na, K, and Mg likely)

Table 5. Tumacacori (To_{18}) Size Fraction Analysis

Size Fraction Mesh Per Inch (U.S. Standard)	Percent of Sample Weight	X-ray Analysis	Remarks
Gravel:			
+4	2.25		Rounded to subangular grains of quartz and weathered granites. Occasional rounded grains of quartzite.
-4 +8	4.35		
Sand:			
-8 +16	9.37		" " "
-16 +30	13.05	Feldspars, quartz, mica	Quartz grains increasing relative to rock fragments
-30 +50	12.05	Feldspars, quartz, mica	Individual feldspar grains and mica flakes, angular quartz. Rock fragments decreasing
-50 +100	8.89	Feldspars, quartz, mica	" " "
-100 +200	8.40	Feldspars, quartz, mica, amphibole	" " "
-200 +270	5.91	" " "	
-270 +400	4.86	" " "	Angular quartz is the dominant mineral
-400 +20μm	11.88	Quartz, feldspars, mica, illite, amphibole	" " "
Silt (-20μm +2μm)	9.07	Quartz, feldspars, mica, illite, amphibole	" " "
Clay (<2μm)	9.02	Quartz, illite, feldspars, montmorillonite	" " "
Organic	0.21		Twigs and grasses
Soluble Salts	0.37		

Table 6. Tumacacori Soil Sample (To_{15}) Size Fraction Analysis

Size Fraction Mesh Per Inch (U.S. Standard)	Percent of Sample Weight	X-ray Analysis
Gravel:		
+4	0.18	
-4 +8	0.97	
Sand:		
-8 +16	0.85	
-16 +30	1.06	Feldspars, quartz, mica
-30 +50	1.64	" " "
-50 +100	1.58	" " "
-100 +200	1.68	Feldspars, quartz, mica amphibole
-200 +270	1.59	" " "
-270 +400	1.10	" " "
-400 +20μm	5.89	" " "
Silt (20μm +2μm)	37.74	Quartz, feldspars, mica, illite (trace), montmorillonite (trace)
Clay (<2μm)	45.54	Quartz, illite, montmotillonite, feldspars, kaolinite, mica
Organic	Nil	
Soluble Salts	0.17	

3.3.4 Soluble Salt Analyses

Soluble salt fractions from four Tumacacori specimens (To_{10}, To_{11}, To_{15} and To_{16}) were separated for qualitative elemental analysis by energy dispersive x-ray analysis. Analytical results are given in Table 7. The elements are listed in decreasing order of elemental abundance.

Table 7. Elemental Analysis of Soluble Salts in Tumacacori Adobe

Specimen Number	Soluble Salt Content as a Percentage of Sample Weight	Analytical Results*
To_{10}	1.26	S, Ca, Cl, K, Si and trace amounts of Mg, Al, and Na
To_{11}	8.78**	Ca, Cl, K, S, Mg
To_{15}	0.17	K, Cl, S, Ca, Si, Mg, and trace amounts of Na, Al, and P
To_{16}	5.78	Ca, K, Mg, Cl, S and a trace amount of Si
To_{18}	0.37	Not analyzed

* Based on three analyses of each specimen.
** As a percent by weight of the -50 mesh fraction

A quantitative analysis of the composition of the salts obtained from Specimen To_{11} was carried out to determine the relative amounts of the major species present. This was accomplished using ion-selective electrodes in combination with gravimetric techniques. The results of this analysis are given in Table 8.

Although the relative amounts of each differed, calcium, sulfur, potassium, and chlorine were observed in all salts, no attempt was made to identify the compounds present by x-ray analysis. However, $CaSO_4 \cdot 2H_2O$ and $CaCl_2$ were identified in specimen To_{11} by SEM-EDXA. The hygroscopic nature of the salts was examined by measuring their weight gains on equilibration with air at 23°C and 35%r.h. after drying to constant weight at 105°C. The salts from sample To_{10} exhibited a weight gain of about 21% while those from To_{11} and To_{16} gained 59% and 63%, respectively. Sufficient water was taken up by the salts from To_{11} and To_{16} to cause them to appear as viscous fluids as illustrated in Figure 11.

Table 8. Analysis of Salts Extracted from Specimen To_{11}

Chemical Species	Weight Percent
K^+	19.5
Na^+	0.6
Mg^{++} and Ca^{++}	16.0
Cl^-	12.4
$SO_4^=$	20.2
H_2O (as water of hydration)≠	31.3

≠ Includes weights of species present in trace amounts.

Gypsum was observed in all of the Tumacacori adobe samples. Small white particles or pore fillings in sample To_{17}, believed to be gypsum, but too fine to be separated were examined by energy dispersive x-ray analysis. An SEM Ca-S map confirmed the presence of gypsum. Figure 12 shows the distribution of these fine particles at 10X magnification. When the gypsum just fills the pores and channels of the adobe, it may leave the matrix undisturbed and in fact have a cementing effect. This was observed in To_{16} which was very well consolidated in spite of being wet. However, when the gypsum crystals greatly exceed the size of the pores, such as in sample To_{11}, they displace the clay-silt matrix in their immediate vicinity and may cause a disruption of the matrix as stresses produced by crystal growth are relieved. Cyclic wetting and drying exacerbate this effect through the dissolution and regrowth of these crystals.

The effects of freeze-thaw damage may also be more severe in the presence of soluble salts. The hygroscopic nature of salts such as $MgCl_2$, $MgSO_4$, or $CaCl_2$ causes the retention of water within the structure. If this water freezes, disrupture effects can occur dur to ice crystallization. In addition, the freezing of water facilitates salt crystallization. As a result, cyclic dissolution and regrowth of salt crystals can occur with changes in temperature as well as with changes in the absolute moisture content within an adobe structure.

The soil sample, To_{15}, and sample To_{18} were found to contain 0.17 and 0.37 wt% soluble salts, respectively, while samples To_{10}, To_{11}, and To_{16} contained much higher salt concentrations (see Table 7). This salt buildup is indicative of the migration of ground water into parts of the structure. Elemental analysis of the salt compositions indicated the presence of gypsum.

This was not unexpected since the nave walls were originally covered with a gypsum wash. However, the high concentrations of gypsum observed in the bulk material indicate the movement of water within the body of the structure. Analyses also revealed the presence of alkalies and chloride ions indicating that rising ground water is carrying these ions into the structure. As this water evaporates, the salts are left behind, either at the surface (efflorescence) or immediately below it (subflorescence). Their presence ultimately leads to severe disruption of the adobe matrix either through crystal growth, as in the case with gypsum, or due to their deliquescence, as in the case with calcium or magnesium chlorides, or both. Both effects occur in certain portions of Tumacacori and appear to be the major cause of deterioration of portions of the interior nave wall.

3.3.4 Summary

The degree of consolidation observed in the various adobe samples from Tumacacori correlated with the concentrations of soluble salts present. Samples taken from a number of locations in the structure were relatively uniform in mineralogical composition and particle size distribution. The soil sample, however, was found to be high in silt and clay, suggesting that the coarser fractions were intentionally added to achieve the desired proportioning. The distinctive feature of Tumacacori adobe is the chemical zoning of the feldspars.

4. POROSITY ANALYSES OF TUMACACORI, FORT BOWIE, AND ESCALANTE RUIN

The weathering of adobe is closely related to the effects of moisture; therefore, the durability of an adobe may be expected to be closely related to its porosity. As a consequence, density and porosity measurements were carried out on selected adobe samples. In addition the particle size distributions in the silt and clay-size fractions were analyzed. Densities were determined by helium pycnometry while porosities were determined using mercury intrusion porosimetry. The density and porosity data are summarized in Table 9, and the pore size distributions are shown in Figure 13. In this figure the percentage of total porosity is plotted as a function of pore diameter. The porosity data presented in Table 9 and Figure 13 are confined to pores with diameters between 177 and 0.0035μm. The nature of the distributions of large diameter pores (voids) in these specimens is mentioned in the preceeding sections.

Table 9. Densities and Porosities of Selected Adobe Samples

Sample Designation	Density grams/cc	Net Pore Volume cc/grams	Average Pore Diameter μm	Measured Total Porosity* %
To_{10}	2.56	0.233	4.2	37.4
To_{11}	2.56	0.213	14.0	34.5
To_{12}	2.60	0.199	2.5	33.9
To_{17}	2.46	0.318	4.8	43.0
Fort Bowie	2.68	0.150	3.4	27.9
Escalante	2.80	0.227	2.8	38.2

*Size range 177 - 0.0035μm

The densities of the adobes listed in Table 9 are somewhat variable, however, densities of the adobe samples from Tumacacori do not vary appreciably, differing at most by 5.7%. Similarly, the average pore diameters observed in these samples does not vary greatly, with the exception of To_{11}. A larger average pore diameter in To_{11} may be attributable to the disruptive affects of salt action. Cyclic dissolution and recrystallization of salt and water in the pores appears to alter the internal porosity distribution; total measured porosity does not appear to increase and may, in fact, decrease dur to space filling by salt crystals.

The total measured porosities of the adobes from the three sites cover a rather broad range from about 28% to 43%. There is not a direct correlation with the degree of weathering. For example, the Fort Bowie corral is severely weathered yet this sample shows the smallest total measured porosity. However, a comparison of the porosities of samples from Tumacacori may be qualitatively correlated. Sample To_{10}, from the top of an exposed wall, and To_{17}, from an exterior location, show the highest measured porosity, yet the porosity from To_{10} which has been subjected to more severe weathering conditions (See Table 10) is lower. It should be pointed out, however, that variations in the original proportioning of these adobes along with the amount of water used would have a significant effect on their total porosities.

The particle size distributions of the samples listed in Table 9 were determined using a sedimentation technique. These analyses were limited to particles which passed a 75μm sieve and were carried out to examine the size distribution within the silt and clay size fractions. Table 10 summarizes the data shown in Figure 14. Figure 14 plots the cumulative mass percent as a function of particle diameter and shows the relative proportions of silt and

clay in addition to the distributions of particle sizes. Reference to the samples from Tumacacori indicates that To_{10} and To_{11} are deficient in clay when compared with To_{12} and To_{17}, but contain relatively larger amounts of silt and fine sand (Table 10). Figure 14 shows samples To_{10} and To_{11} to be devoid of clay particles with diameters below about 1.1μm. This indicates that the weathering of these samples is primarily reflected in the loss of fine clay particles, while their relatively high silt contents may indicate that particles in this size range are less sensitive to the action of water.

Table 10. Particle Size Distribution by Sedimentation

Sample Designation	% Sand -75 +20μm	% Silt -20μm +2μm	% Clay -2μm
To_{10}	22	71	7
To_{11}	10	78	12
To_{12}	14	61	25
To_{17}	6	66.5	27.5
Fort Bowie	17	61	22
Escalante	18	55	27

5. SUMMARY AND CONCLUSIONS

Adobe from Escalante Ruin was found to be well consolidated in spite of its high soluble salt content. The high degree of consolidation along with the light color of this material is attributable to the presence of massive amounts of calcite which behaves both as a cementing agent and a pigment.

The adobe from Fort Bowie National Historic Site has a low soluble salt content but exhibits poor resistance to weathering. This was found to be the result of the particle size distribution since this adobe contains a large fraction of gravel and coarse sand but is deficient in the fine, bonding fractions.

The adobe from Tumacacori National Monument showed varying degrees of consolidation. A series of samples from an interior wall showed variable consolidation which was dependent on their soluble salt contents. The presence of soluble salts is indicative of rising ground water and those samples with high salt concentrations showed signs of significant deterioration. Other samples in which less salt was present showed a high degree of consolidation. One sample from an exterior wall was well consolidated in spite of the fact that the action of rain had leached out a significant amount of its fine clay fraction.

An analysis of the salts present in one deteriorated sample revealed the presence of chlorides and sulfates of calcium and magnesium; of these $MgCl_2$, $MgSO_4$ and $CaCl_2$ are hygroscopic salts. The tendency of the salts to retain water leads to deterioration through several processes including cyclic wetting and drying, cyclic salt recrystallization, and freeze-thaw damage.

A comparison of the particle size distribution of a soil sample from the Tumacacori site with those of several samples from the structure suggested that the adobe was deliberately proportioned for use in construction. The church at Tumacacori was built with adobe apparently composed of 1 part of soil diluted with about 4 parts of sand.

Based on the analyses carried out on the adobe from the three sites investigated, it was possible to correlate the type and severity of weathering observed with compositional, particle size distribution, porosity, and soluble salt analyses. Analyses of the mineralogical aspects of the samples studied allowed an assessment of their variability while indicating that the deterioration observed in these samples did not result from the presence of a swelling clay. The combination of these analyses also provides a basis for the selection of adobe repair material which would be representative of that originally used.

6. REFERENCES

1. J. R. Clifton, Preservation of Historic Adobe Structures - A Status Report, NBS Tech. Note 934, U.S. GPO (1977).

2. J. R. Clifton, P. W. Brown, and C. R. Robbins, Methods for Characterizing the Physicochemical Properties of Adobe Building Materials, NBS Tech. Note. In press.

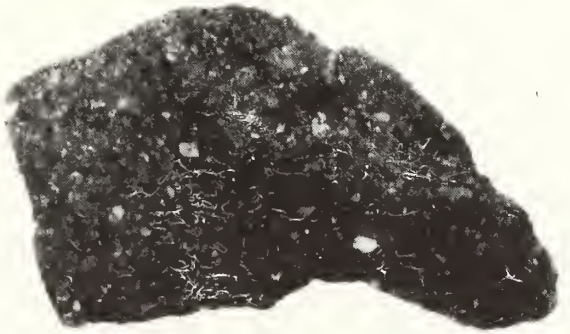

TUMACACORI

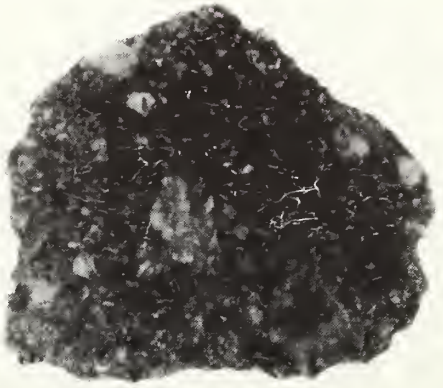

FORT BOWIE

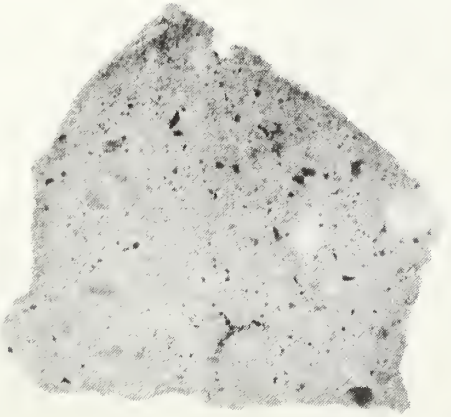

ESCALANTE

Figure 1. Epoxy-impregnated polished sections of adobe samples from Tumacacori, Fort Bowie, and Escalante. The general aspects of color and void and aggregate distribution may be observed.

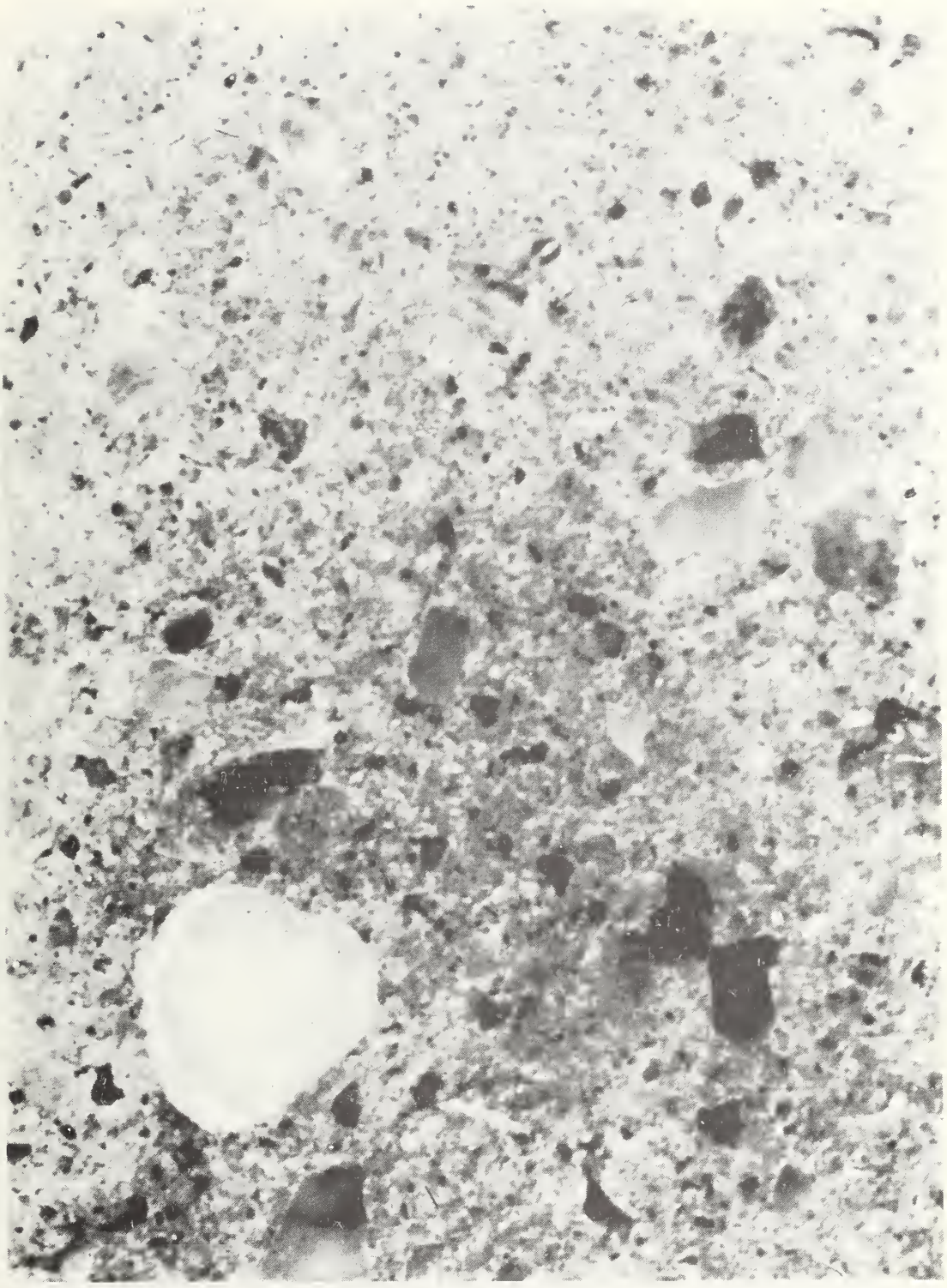

Figure 2. Epoxy-impregnated polished section of adobe from Escalante showing the aggregate distribution in the fine matrix. The light color of the matrix is due to the presence of calcite. 10X magnification.

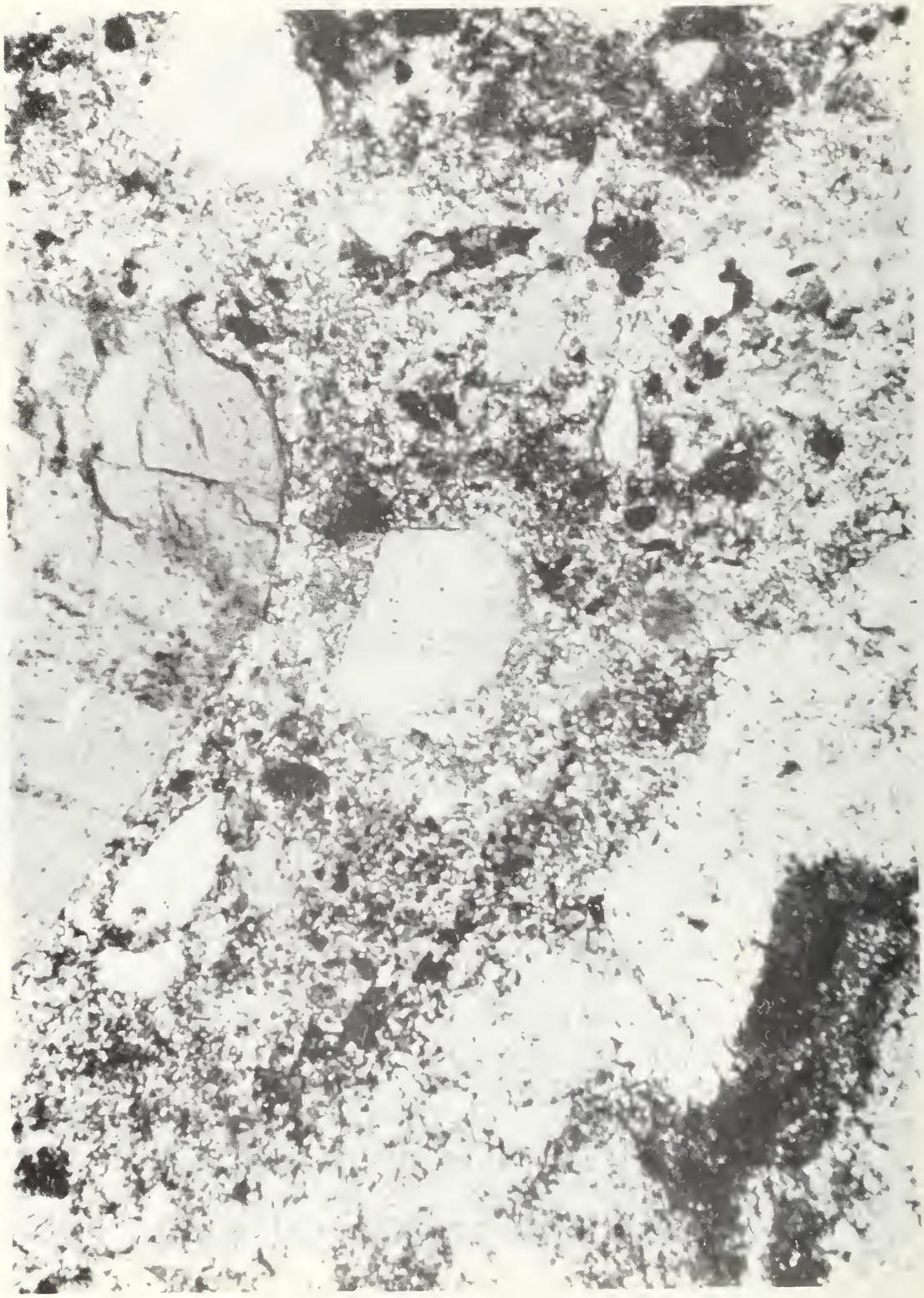

Figure 3. Thin section of adobe from Escalante viewed in transmitted polarized light showing coarse quartz and feldspar grains in their characteristic calcite-clay matrix. 100X magnification

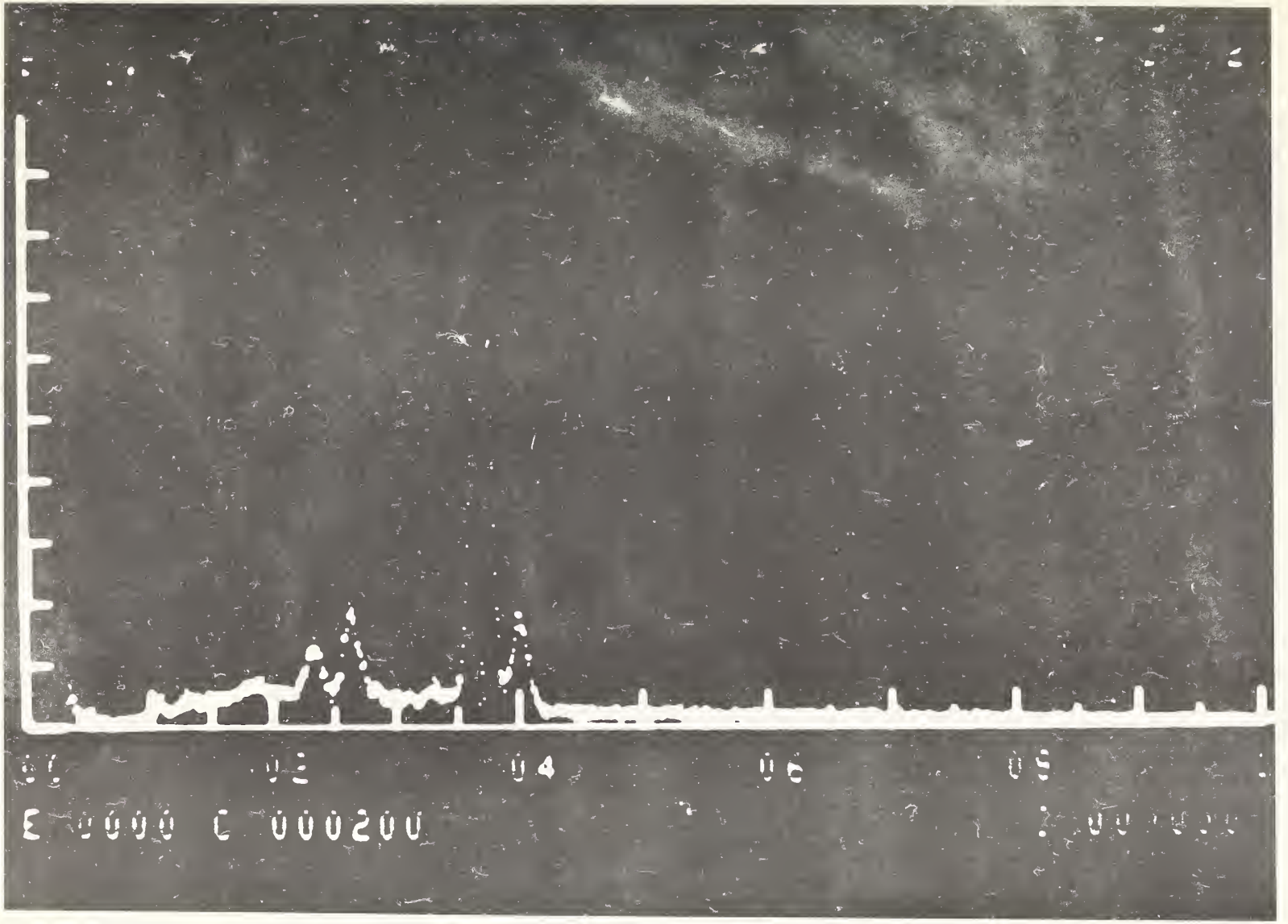

Figure 4. Energy distribution spectrum of the soluble salts extracted from Escalante adobe. Ca > Cl > S. Trace amounts of Mg, K, and Al are also observed.

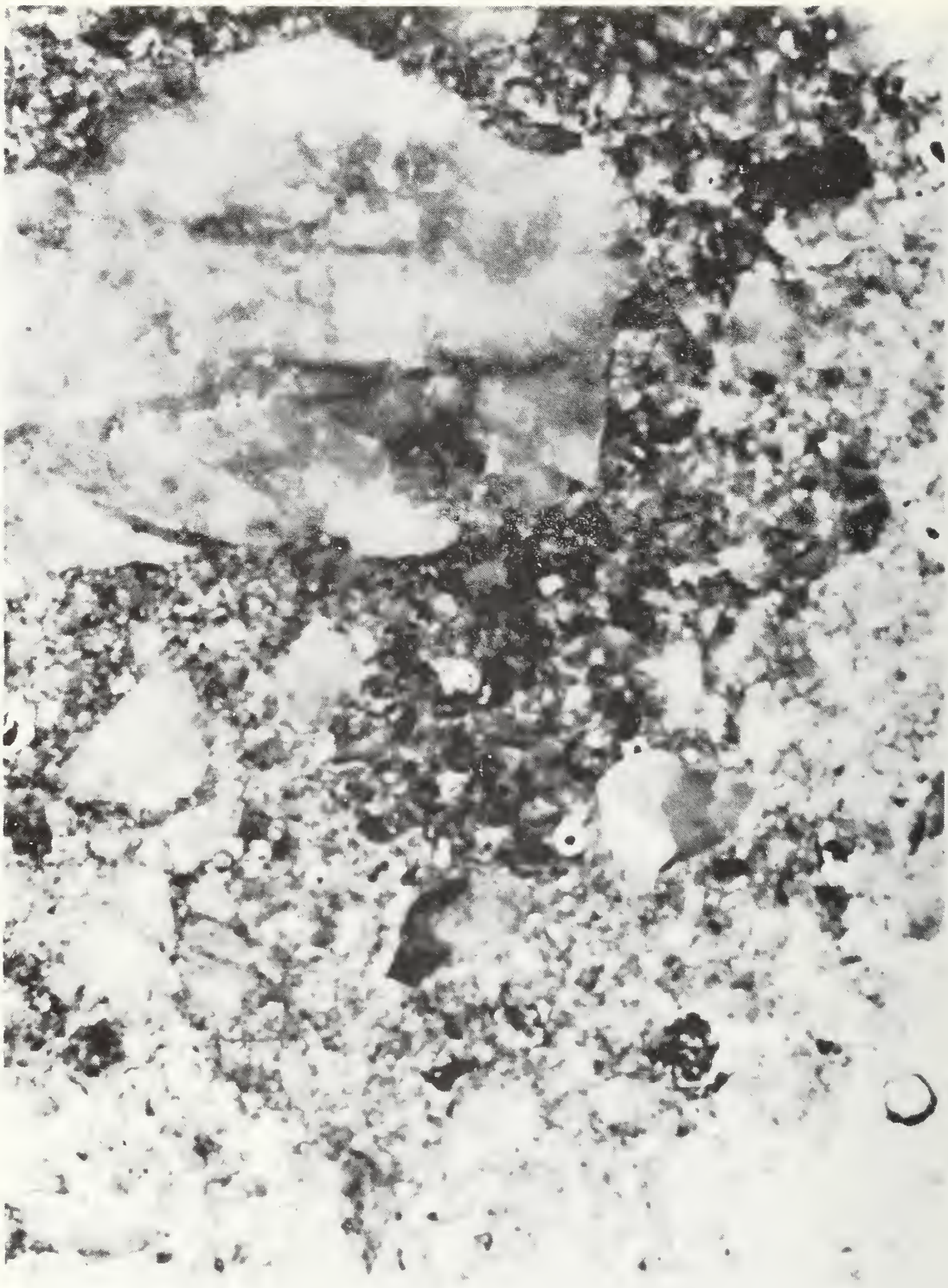

Figure 5. Epoxy-impregnated polished section of adobe from Fort Bowie showing the distribution of aggregate in the matrix. 10X magnification. The size of the aggregate in this adobe as compared to that in Escalante (Figure 2) or Tumacacori (Figure 8) is noteworthy.

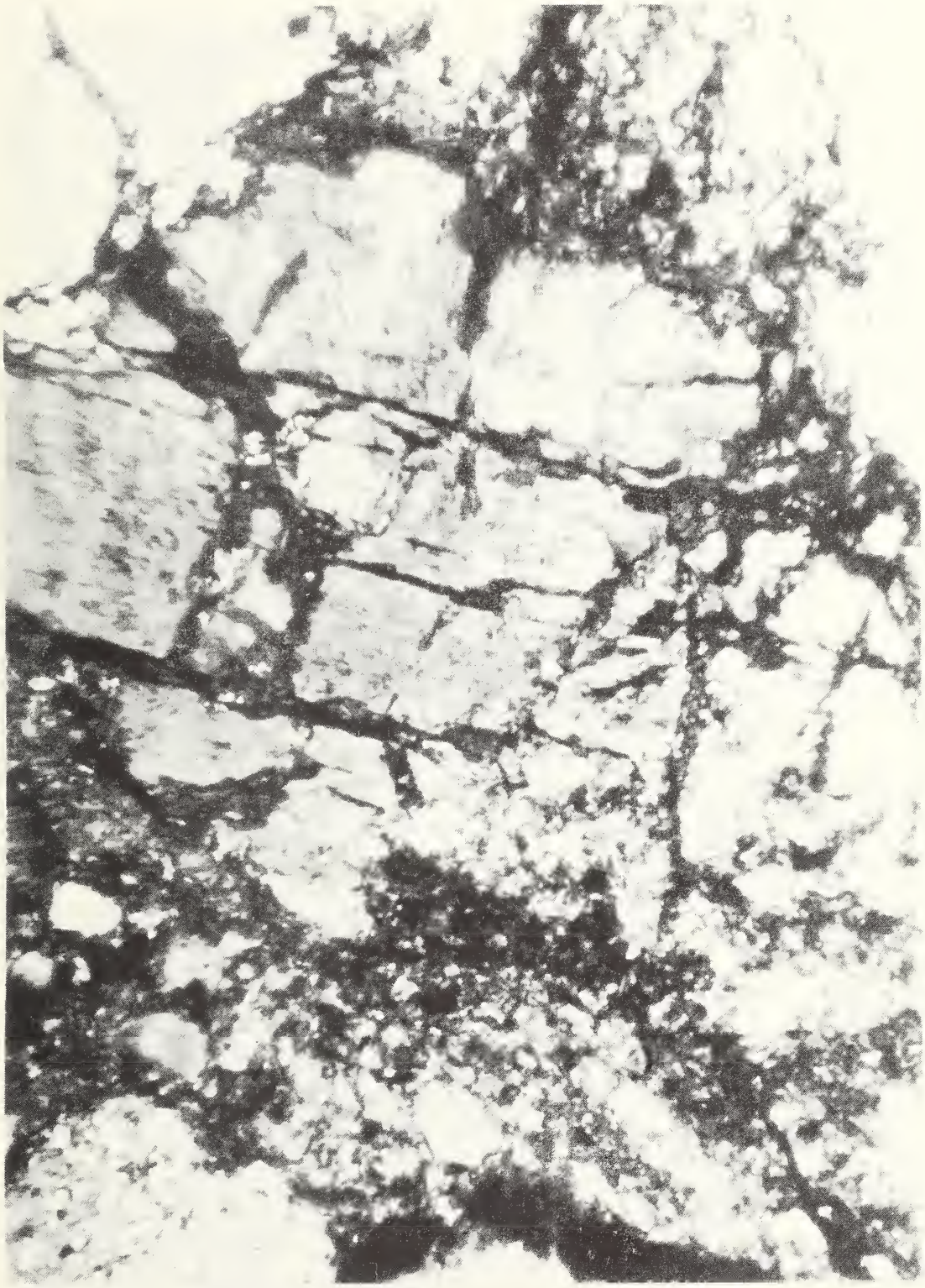

Figure 6. Thin section of adobe from Fort Bowie viewed in transmitted polarized light showing large aggregate grains separated by narrow regions of silt-clay matrix. 50X magnification. This feature is distinctive of this adobe.

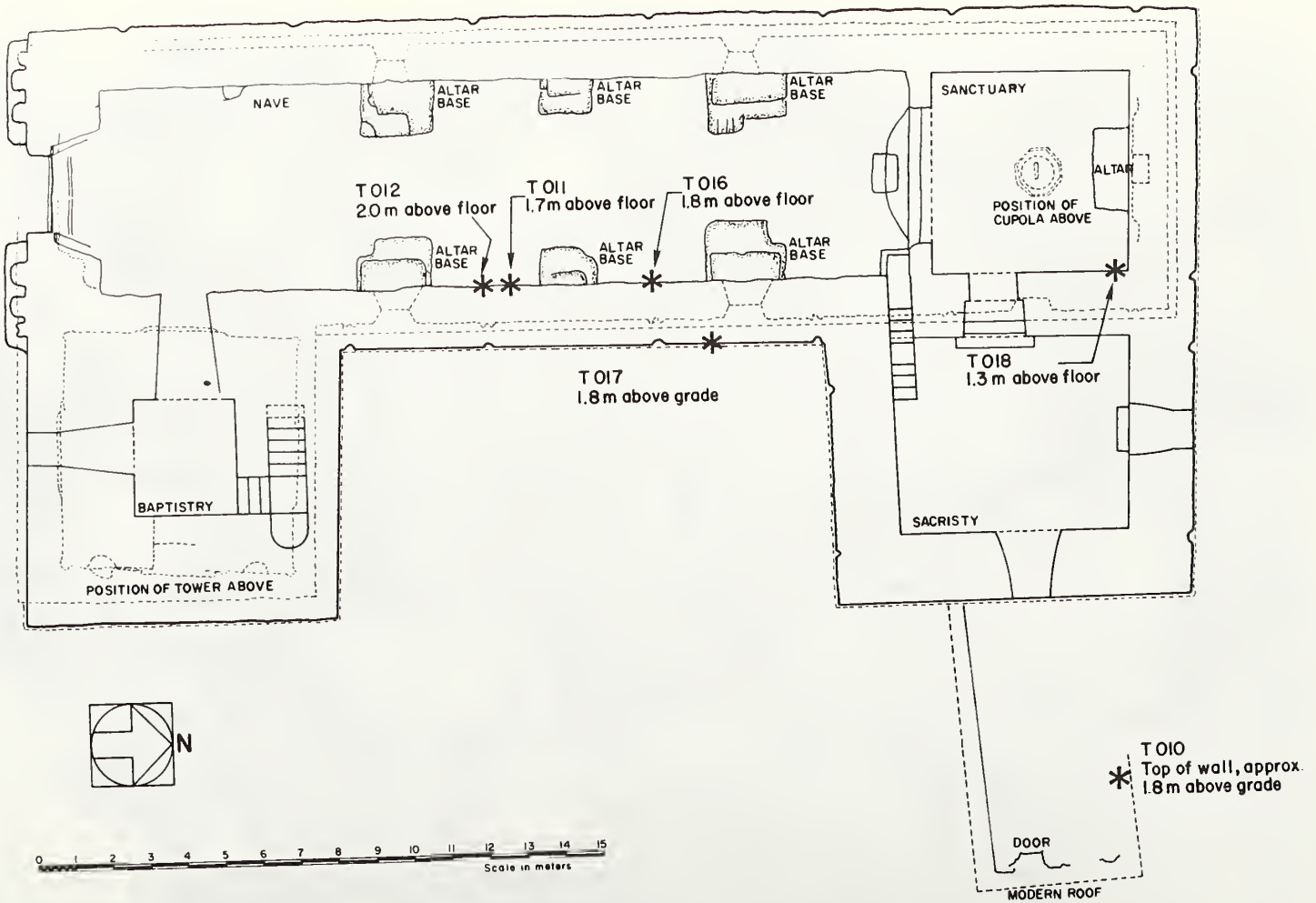

Figure 7. A map of Tumacacori National Monument showing the sampling locations.

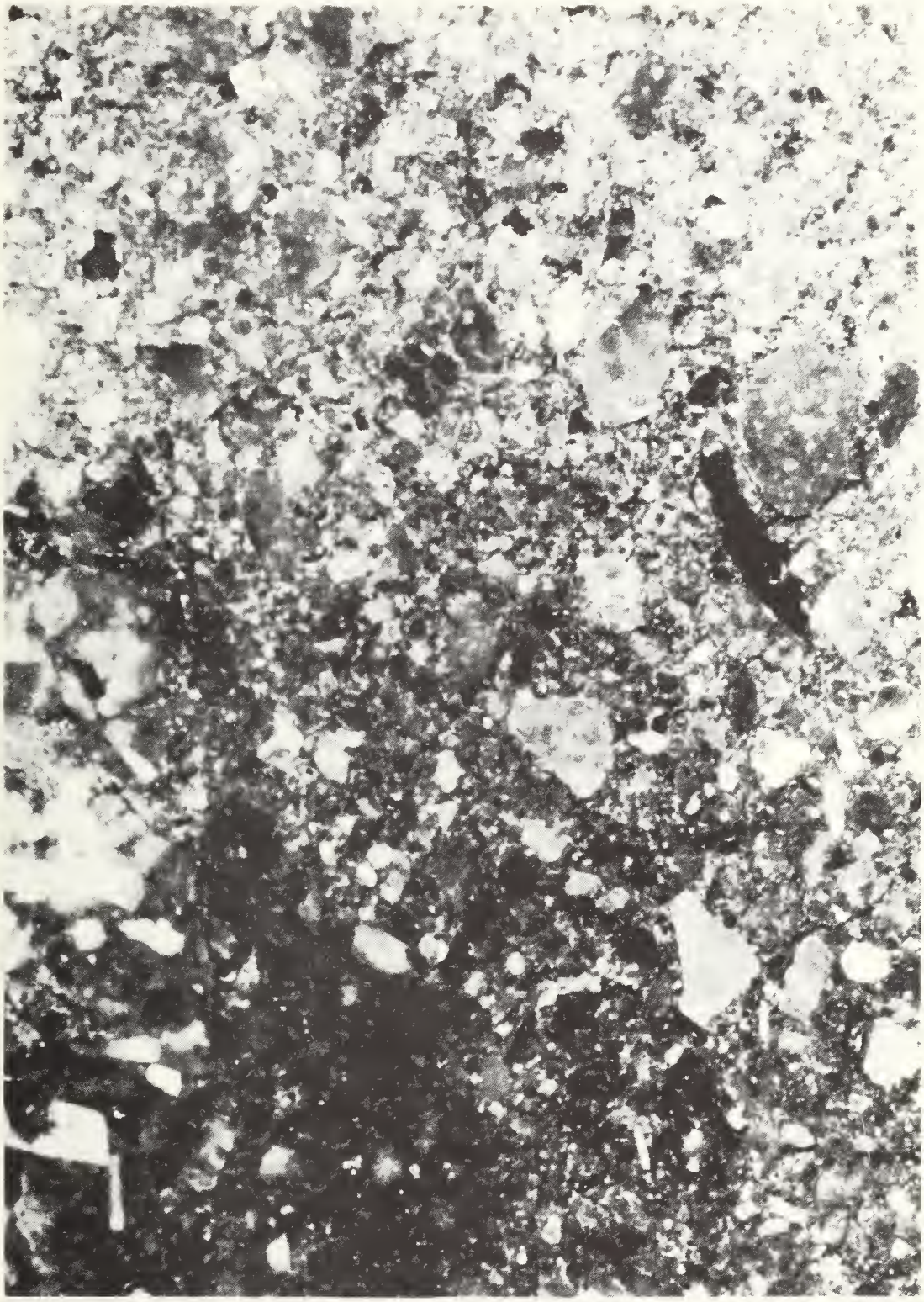

Figure 8. Epoxy-impregnated polished section of adobe from Tumacacori showing the distribution of aggregate in the fine matrix. 10X magnification.

Figure 9. Epoxy-impregnated fracture surface of adobe from Tumacacori showing deposits of gypsum (white) filling the pores. 10X magnification. Sample To_{11}.

Figure 10. Thin section of adobe from Tumacacori showing a chemically zoned feldspar crystal in the silt-clay matrix. Such zoning is common in the detrital feldspars of this locality. Transmitted polarized light. 100X magnification.

Figure 11. Soluble salts extracted from Tumacacori specimen To_{11}. This salt sample was dryed at 105°C to constant weight and then exposed to laboratory air (23°C, 35% r.h.) for 30 minutes. 65X magnification. Transmitted polarized light.

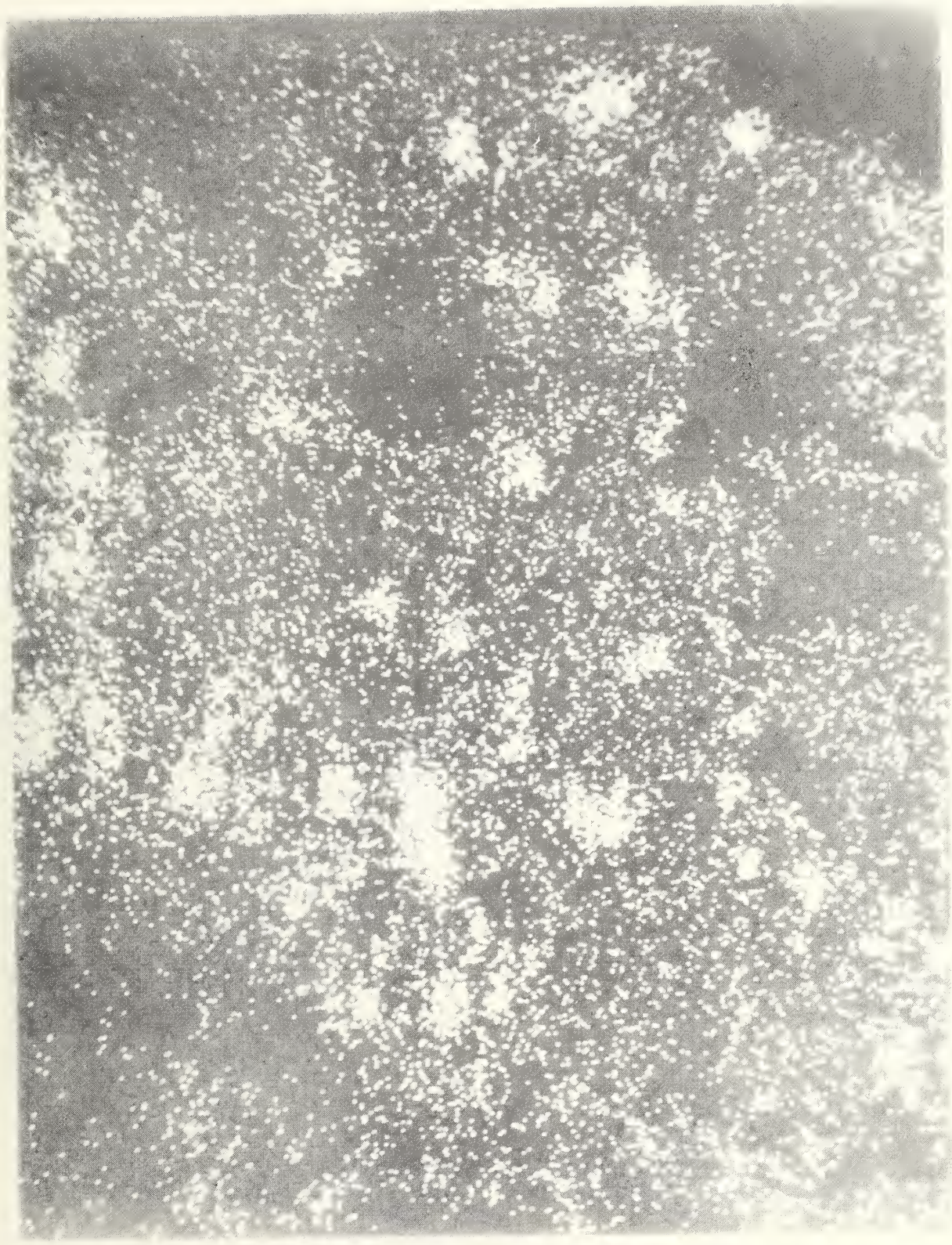

Figure 12. An energy dispersive x-ray map of the calcium and sulfur distribution in Tumacacori specimen To_{17}. This shows the distribution of the gypsum particles (white areas) in this specimen. 10X magnification.

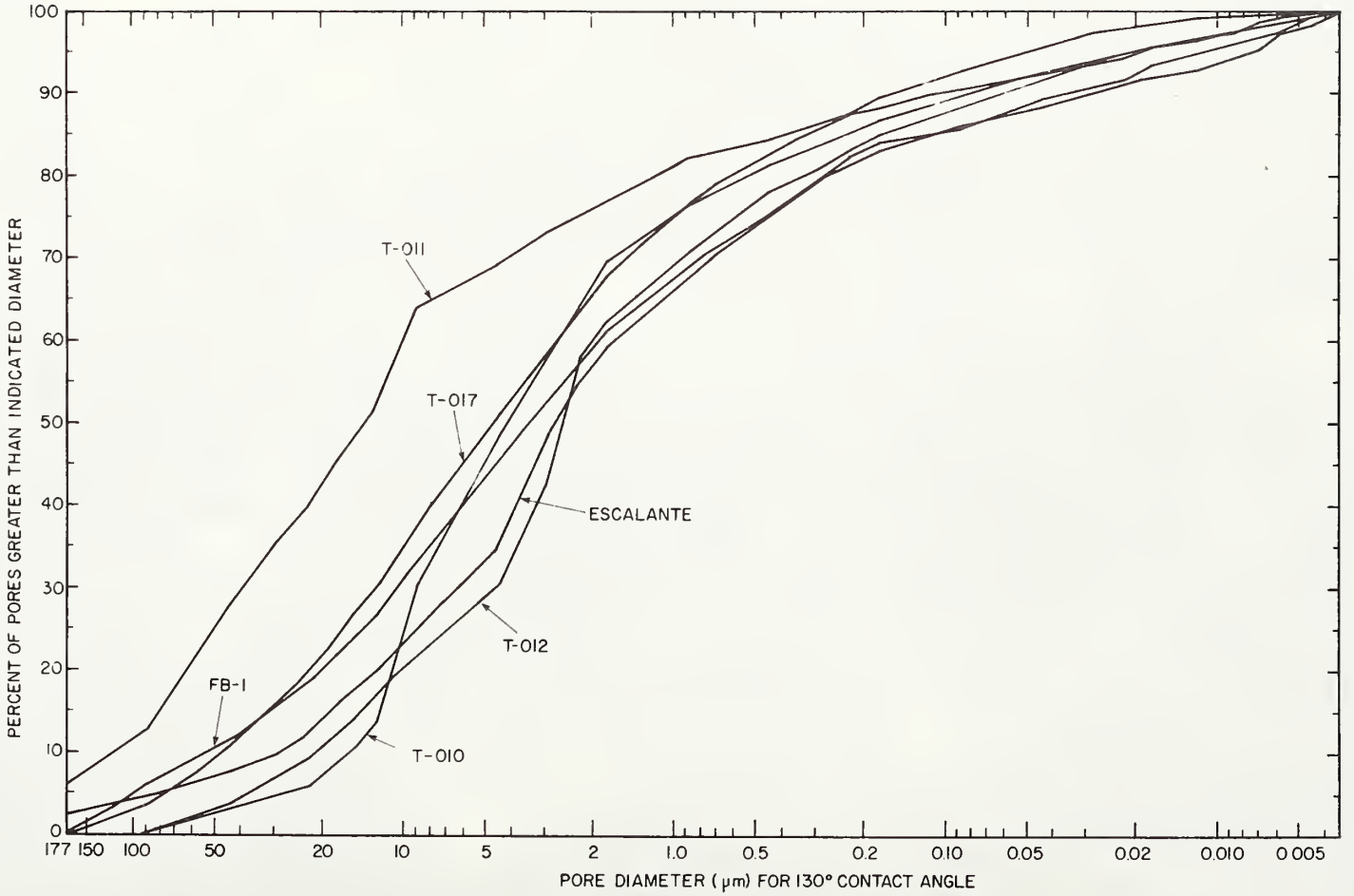

Figure 13. The porosity distributions in Tumacacori samples To_{10}, To_{11}, To_{12} and To_{17} and in the Escalante and Fort Bowie samples for the pore sizes from 177 to 0.0035μm. The Tumacacori sample To_{11} is shown to have a significantly higher porosity for pore diameters larger than about 1μm.

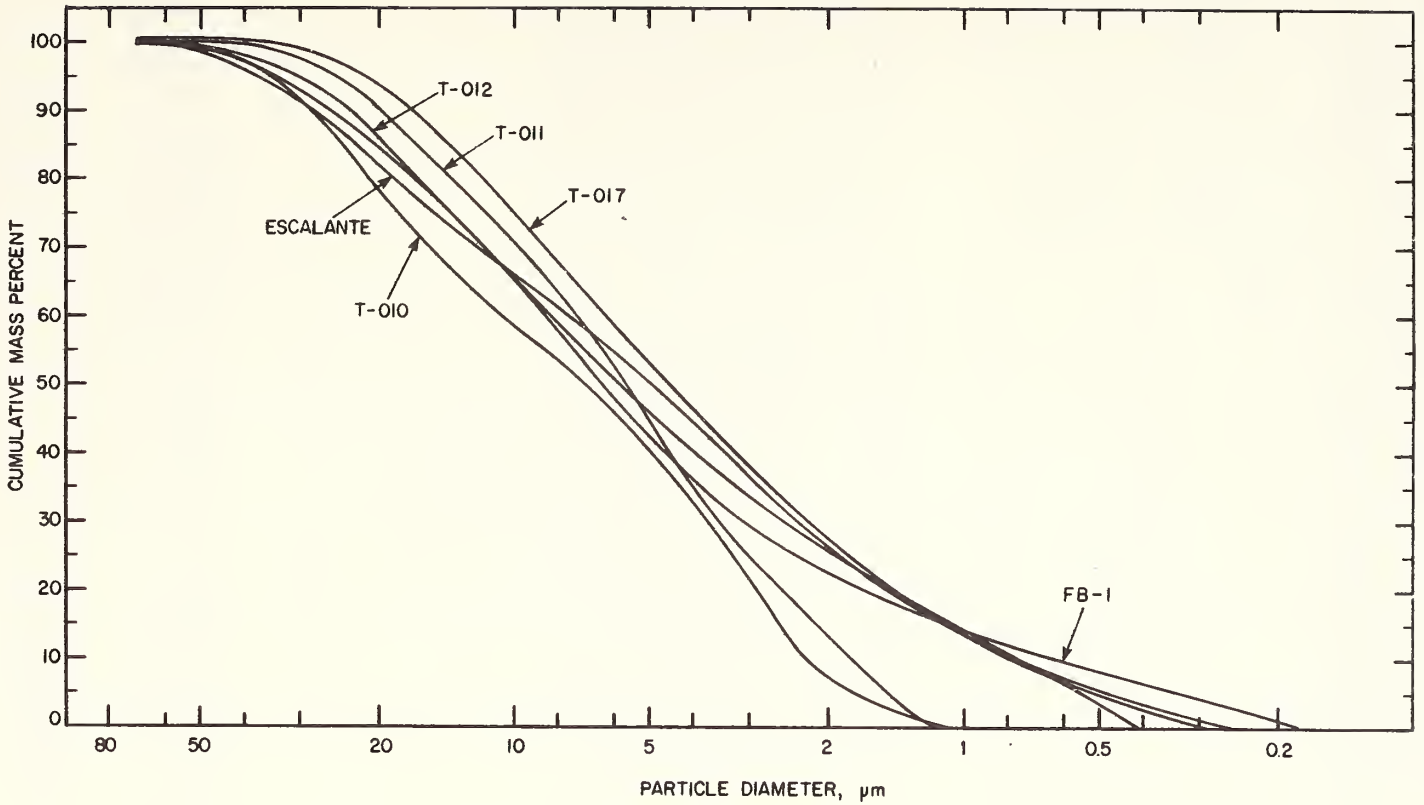

Figure 14. The size distributions of particles with diameters smaller than 75μm in Tumacacori samples To_{10}, To_{11}, To_{12}, and To_{17} and in the Escalante and Fort Bowie samples. The relative distributions of silt (-20+2μm) and clay (-2μm) size particles may be seen. Tumacacori samples To_{10} and To_{11} are shown to be deficient in their fine clay fractions.

8. ACKNOWLEDGMENT

The authors wish to acknowledge the financial support of the Western Archeological Center of the National Park Service. In particular they wish to express their sincere thanks to George Cattanach, Dennis Fenn and Anthony Crosby of the National Park Service for their technical and administrative assistance.

NBS-114A (REV. 7-73)

U.S. DEPT. OF COMM. BIBLIOGRAPHIC DATA SHEET	1. PUBLICATION OR REPORT NO. NBSIR 78-1495	2. Gov't Accession No.	3. Recipient's Accession No.

4. TITLE AND SUBTITLE

FACTORS AFFECTING THE DURABILITY OF ADOBE STRUCTURES

5. Publication Date: July 1978

6. Performing Organization Code

7. AUTHOR(S) Paul Wencil Brown, Carl R. Robbins, James R. Clifton

8. Performing Organ. Report No.

9. PERFORMING ORGANIZATION NAME AND ADDRESS

NATIONAL BUREAU OF STANDARDS
DEPARTMENT OF COMMERCE
WASHINGTON, D.C. 20234

10. Project/Task/Work Unit No.

11. Contract/Grant No.

12. Sponsoring Organization Name and Complete Address *(Street, City, State, ZIP)*

National Park Service
Washington, DC 20234

13. Type of Report & Period Covered

14. Sponsoring Agency Code

15. SUPPLEMENTARY NOTES

16. ABSTRACT *(A 200-word or less factual summary of most significant information. If document includes a significant bibliography or literature survey, mention it here.)*

Adobe samples from three sites of historic interest in the State of Arizona were analyzed to determine their mineral assemblages, particle size distributions, soluble salt contents, and porosities. These analyses were accompanied by microscopic observations of polished sections and thin sections. These data were correlated with the weathering observed and it was found that soluble salt action was responsible for the deterioration of the adobe from one of the sites. The nature of the particle size distribution has resulted in the rapid deterioration of the adobe from a second site. The adobe from a third site was found to be well consolidated due to the presence of large amounts of calcite.

17. KEY WORDS *(six to twelve entries; alphabetical order; capitalize only the first letter of the first key word unless a proper name; separated by semicolons)*

Adobe; clay; particle size distribution; soluble salt analysis; weathering; x-ray analysis.

18. AVAILABILITY [XX] Unlimited

[ ] For Official Distribution. Do Not Release to NTIS

[ ] Order From Sup. of Doc., U.S. Government Printing Office Washington, D.C. 20402, SD Cat. No. C13

[x] Order From National Technical Information Service (NTIS) Springfield, Virginia 22151

19. SECURITY CLASS (THIS REPORT) UNCLASSIFIED

21. NO. OF PAGES 40

20. SECURITY CLASS (THIS PAGE) UNCLASSIFIED

22. Price $4.50

USCOMM-DC 29042-P74